Effect of chemical structure of bipyridinium salts as electron carrier on the visible-light induced conversion of CO_2 to formic acid with the system consisting of water-soluble zinc porphyrin and formate dehydrogenase

Yutaka Amao,[a,b,c *] Ryutaro Abe[d], Sachina Shiotani[d]

[a] Advanced Research Institute for Natural Science and Technology, Osaka City University, Sugimoto 3-3-138, Sumiyoshi-ku, Osaka 558-8585, Japan.

[b] Research Centre for Artificial Photosynthesis (ReCAP), Osaka City University, Sugimoto 3-3-138, Sumiyoshi-ku, Osaka 558-8585, Japan.

[c] Precursory Research for Embryonic Science and Technology (PRESTO), Japan Science and Technology Agency, 4-1-8 Honcho Kawaguchi, Saitama 332-0012, Japan

[d] Department of Applied Chemistry, Oita University, Dannoharu 700, Oita 870-1192, Japan

Corresponding Author: Y. Amao

Fax: +81 6 6605 3726; Tel: +81 6 6605 3726; E-mail: amao@ocarina.osaka-cu.ac.jp

© 2015. This manuscript version is made available under the Elsevier user license
http://www.elsevier.com/open-access/userlicense/1.0/

Abstract

Effect of chemical structures of some 2,2'-bipyridinium salts (BP^{2+}) as the electron carrier molecules on the visible-light induced conversion of CO_2 to formic acid with the system consisting of water-soluble zinc tetraphneylporphyrin tetrasulfonate (ZnTPPS) and formate dehydrogenase (FDH) in the presence of triethanolamine (TEOA) as an electron donor molecule was investigated. Irradiation of a CO_2 saturated solution containing TEOA, ZnTPPS, BP^{2+} and FDH with visible light resulted in production of formic acid. By using 1,1'-ethylene-2,2'-bipyridinium dibromide (DB^{2+}) as an electron carrier molecule, the effective formic acid production was observed compared with the other 2,2'-bipyridinium salt derivatives.

Keywords. Artificial photosynthesis, Bipyridinium salt, CO_2 reduction, Formate dehydrogenase, Formic acid synthesis, Zinc porphyrin

1. Introduction

Photoredox system consisting of an electron donating molecule, a photosensitizer, an electron carrier molecule and catalyst is widely used for the photoenergy conversion to chemical energy system [1-5]. This system so called artificial photosynthesis is a simplification of the photoinduced electron transfer process in natural photosynthesis reaction. By using reduced electron carrier molecule as a substrate or coenzyme for the catalyst or enzyme in this system, hydrogen production and CO_2 to the organic material conversion systems would be developed. For visible light-induced hydrogen production systems, platinum nano-particle or enzyme hydrogenase has been used as hydrogen producing catalyst with the visible light sensitizers such as water soluble zinc porphyrins, ruthenium polypyridyl coordination complexes and chlorophyll-*a*[6-18]. The visible light induced chemical and enzymatic synthesis of organic compounds has also been developed using this system in the presence of various dehydrogenases such as lactate (LDH), formate (FDH), aldehyde (AldDH) and alcohol dehydrogenase (ADH) for the synthesis of valuable organic compounds such as lactic acid [19], formic acid [20-28], methanol [29-30] *etc*. Among these dehydrogenases, FDH catalyzes the conversion of CO_2 to formic acid in the presence of a suitable electron donating molecules as a coenzyme such as NADH, reduced form of bipyridinium salts and so on. Thus, visible light-induced CO_2 conversion to organic material system will be developed with the combination of photoredox system and FDH as an artificial photosynthesis model.

Photochemical and enzymatic formic acid synthesis from CO_2 (hydrogen carbonate ion) with formate dehydrogenase (FDH) and methylviologen (MV^{2+}) photoreduction with a system containing ruthenium(II) coordination compound e.g. trisbipyridinium ruthenium (III) $[Ru(bpy)_3]^{2+}$as a photosensitizer and mercaptoethanol (RSH) as an electron donor has been reported for the first time [20-23]. In contrast, we previously reported the photochemical and enzymatic formic acid synthesis from CO_2 or hydrogen carbonate ion with the system consisting of MV^{2+}, FDH and water-soluble zinc porphyrin [25-27] or chlorophyll-*a*[28] in the presence of triethanolamine (TEOA) as an electron donor. To improve the yield of formic acid from CO_2 in the system consisting of a photosensitizer, an electron carrier molecule and FDH, an effective electron carrier molecule for activation of FDH activity of CO_2 to formic acid conversion is desirable. 2,2'-Bipyridinium salt derivatives also act as the effective electron carrier molecules for the formic acid production from CO_2 in the system consisting of a photosensitizer, an electron carrier molecule and FDH instead of MV^{2+}. By using 1,1'-alkyl-2,2'- bipyridinium salt or 1,1'-dimethyl-2,2'- bipyridinium salt, the redox potential and dihedral angle between pyridine rings will be controlled by the methylene chain length bridged between pyridine rings in bipyridinium salt.

In this work, effect of chemical structures of 2,2'-bipyridinium salt derivatives (chemical structures in Fig. 1) as the electron carrier molecules on the visible-light induced conversion of CO_2 to formic acid with the system consisting of water-soluble zinc tetraphneylporphyrin tetrasulfonate

(ZnTPPS) and FDH in the presence of TEOA as an electron donor molecule (Fig. 2) was investigated. By using 1,1'-ethylene-2,2'-bipyridinium dibromide (DB^{2+}) as an electron carrier molecule, the effective formic acid production observed compared with the other 1,1'-alkyl-2,2'-bipyridinium salt derivatives.

2. Experimental

2.1. Materials

FDH from *Candida boidinii* was purchased from Roche Diagnostics K.K. In accordance with the literature, the molecular weight of FDH from *Candida boidinii* was estimated to be 74 kDa. MV^{2+}, tetraphenylporphyrin tetrasulfonate (H_2TPPS), TEOA, 2,2'-bipyridine, methyl iodide, 1,2-dibromoethane, 1,3-diboromopropane and 1,4-dibromobutane were supplied by Tokyo Kasei Co. Ltd. The other chemicals were analytical grade or the highest grade available.

2.2. Preparation of zinc tetraphenylporphyrin tetrasulfonate (ZnTPPS)

Zinc tetraphenylporphyrin tetrasulfonate (ZnTPPS) was synthesized by refluxing H_2TPPS with about 10 times molar equivalent of zinc acetate in 100 ml of methanol at 40 ºC for 2 h. The insert of zinc ion into H_2TPPS was monitored by UV-visible absorption spectra using Shimadzu Multispec 1500 spectrophotometer. During the reaction, the characteristic absorption band of ZnTPPS at 550

nm increased and the absorbance at 650 nm of H_2TPPS decreased gradually. After evaporation of the solvent, the product was dissolved in distilled water. The purification of ZnTPPS was carried out by dialysis (pore diameter of the tube 2.0 nm) in distilled water. UV-vis absorption spectrum of ZnTPPS in an aqueous solution was shown in Fig. 3. The molar coefficients for ZnTPPS also were indicated in Fig. 3. The absorption spectrum shows a typical Soret band with peak at 422 nm as well as Q-band at 555 and 590 nm.

Although small amount of zinc acetate was not removed from ZnTPPS solution, it has been confirmed that zinc acetate has no influence on the following photoreactions [7,8]. Moreover, the photo-stability of ZnTPPS was checked as a following experiment. The solution of ZnTPPS (10 μM) in 3.0 ml of 1.0 mM sodium pyrophosphate buffer (pH 7.4) was deaerated by freeze-pump-thaw cycles repeated 6 times. The sample solution was irradiated with a 250 W halogen lamp at a distance of 3.0 cm with a Toshiba L-39 cut-off filter at 30 ˚C. The degradation of ZnTPPS was determined by the absorbance at 422 nm using the molar coefficient. For 7 h continuous irradiation, little change of the absorbance at 422 nm was observed. Thus, ZnTPPS has a good stability for continuous irradiation.

2.3. Preparation of 2,2’-bipyridinium salt derivatives

1,1’-Alkyl-2,2’-bipyridinium salts was synthesized by following method as shown in Scheme 1-1. 2,2’-Bipyridine (10 mmol) was dissolved in 300 ml of acetonitrile and then *α, ω*-dibromoalkane (*n*=2-4) (100 mmol) was added to the reaction mixture with stirring at 100 °C for 48 h. 1,1’-Alkyl-2,2’-bipyridinium salt was produced as a bright yellow precipitate. The precipitate was collected by suction filtration and washed with acetonitrile. The desired product was recrystallized from ethanol and water and dried under vacuum overnight. Proton nuclear magnetic resonance (^{1}H-NMR) in D_2O: δ (ppm) 1,1’-ethylene-2,2’-bipyridinium dibromide (DB^{2+}): 4.78 (s, 6H), 7.95 (m, 2H), 8.10 (m, 2H), 8.78 (m, 2H), 9.02 (m, 2H). 1,1’-trimethylene-2,2’-bipyridinium dibromide (TB^{2+}): 2.59 (s, 2H), 4.37 (s, 4H), 7.94 (m, 2H), 8.08 (m, 2H), 8.78 (m, 2H), 9.20 (m, 2H). 1,1’-tetramethylene-2,2’-bipyridinium dibromide (QB^{2+}): 2.07 (s 4H), 4.59 (s, 4H), 7.93 (m, 2H), 8.06 (m, 2H), 8.79 (m, 2H), 9.02 (m, 2H). ^{1}H-NMR spectra were recorded on a Varian GEMINI-200. The chemical shifts were referenced to the solvent peak calibrated against tetramethylsilane (TMS).

1,1’-Dimethyl-2,2’-bipyridinium salt (DM^{2+}) was synthesized by following method as shown in Scheme 1-2. 2,2’-Bipyridine (17.6 mmol) was dissolved in 300 ml of acetonitrile and then methyliodide (176 mmol) was added to the reaction mixture with stirring at 100 °C for 48 h. 1,1’-Dimethyl-2,2’-bipyridinium salt was produced as a bright yellow precipitate. The precipitate was collected by suction filtration and washed with acetonitrile. The desired product was

recrystallized from ethanol and water and dried under vacuum overnight. ^{1}H-NMR in D_2O: δ (ppm) DM^{2+}: 4.23 (s, 6H), 7.94 (m, 2H), 8.07 (m, 2H), 8.78 (m, 2H), 9.02 (m, 2H).

2.4. Determination of molar coefficient for reduced form of 2,2'-bipyridinium salt derivatives

Molar coefficients for reduced form of 2,2'-bipyridinium salt derivatives were determined by following method. A solution containing 2,2'-bipyridinium salt derivative (0.1 mM) and sodium dithionite (0.1 M) in distilled water was deaerated with argon gas bubbling for 5 min. The production of reduced form of 2,2'-bipyridinium salt derivative was monitored by UV-vis absorption spectrum using Shimadzu Multispec 1500 spectrophotometer. Molar coefficients for reduced form of 2,2'-bipyridinium salt derivative was determined by the absorbance of maximum in absorption spectrum using Beer-Lambert law.

2.5. Redox potential measurement of 2,2'-bipyridinium salt derivatives

The redox potentials for 2,2'-bipyridinium salt derivatives were determined by cyclic voltammetry (Hokuto Denko HZ-3000). All measurements were carried out under nitrogen-saturated solution containing 0.2 M potassium chloride and 1.0 mM sodium pyrophosphate buffer (pH 7.4) at a carbon-working electrode. A platinum wire was used as a counter electrode. All potentials were relative to the Ag/AgCl electrode used as the reference.

2.6. Photoreduction of 2,2’-bipyridinium salt derivatives by photosensitisation of ZnTPPS

A solution containing ZnTPPS (10 μM), 2,2’-bipyridinium salt derivative (0.1 mM) and TEOA (0.3 M) as an electron donor molecule in 3.0 ml of 1.0 mM sodium pyrophosphate buffer (pH 7.4) was deaerated by freeze-pump-thaw cycles repeated 6 times. The sample solution was irradiated with a 250 W halogen lamp at a distance of 3.0 cm with a Toshiba L-39 cut-off filter at 30 ˚C. Reduced 2,2’-bipyridinium salt derivative concentration was determined by the absorbance at 605 nm using the molar coefficient.

2.7. Visible light-induced formic acid synthesis form CO_2 with ZnTPPS, 2,2’-bipyridinium salt derivatives and FDH

A solution containing ZnTPPS (10 μM), 2,2’-bipyridinium salt derivative (0.1 mM), TEOA (0.3 M) and FDH (9.3 μM) in 3.0 ml of 1.0 mM sodium pyrophosphate buffer (pH 7.4) was deaerated by freeze-pump-thaw cycles repeated 6 times and then flushed with CO_2 gas for 5 min. The sample solution was irradiated with a 250 W halogen lamp and wavelengths of less than 390 nm were blocked with a cut-off filter at 30 ˚C. The amount of formic acid produced was detected by an ionic chromatograph system (Dionex IC2000).

3. Results and Discussion

3.1. Molar coefficient for reduced form of 2,2'-bipyridinium salt derivatives

Molar coefficients for dithionite reduced 2,2'-bipyridinium salt derivatives were determined by UV-vis absorption spectra. Molar coefficients for reduced DB^{2+}, TB^{2+}, QB^{2+} and DM^{2+} were estimated to be 4313.5 (λ_{max}: 450 nm), 1253.9 (λ_{max}: 450 nm), 4132.8 (λ_{max}: 436 nm) and 2166.8 $M^{-1}cm^{-1}$ (λ_{max}: 436 nm), respectively.

3.2. Redox potential for 2,2'-bipyridinium salt derivatives

Redox potentials for 2,2'-bipyridinium salt derivatives were determined by cyclic voltammetry using Ag/AgCl electrode as the reference. The first reduction potentials for DB^{2+}, TB^{2+}, QB^{2+} and DM^{2+} were estimated to be -0.65, -0.82, -0.92 and -0.99 V (*vs* Ag/AgCl), respectively. The first oxidation potentials for DB^{2+}, TB^{2+}, QB^{2+} and DM^{2+} were estimated to be -0.45, -0.62, -0.72 and -0.79 V (*vs* Ag/AgCl), respectively. Thus, the redox potentials ($E_{1/2}$) for DB^{2+}, TB^{2+}, QB^{2+} and DM^{2+} were calculated to be -0.55, -0.72, -0.82 and -0.89 V (*vs* Ag/AgCl), respectively.

3.3. Photoreduction of 2,2'-bipyridinium salt derivatives with visible-light sensitization of ZnTPPS

When the reaction mixture containing ZnTPPS, bipyridinium salt derivative (BP^{2+}) and TEOA was irradiated with visible light, the absorbance attributed to the absorption band of reduced BP^{2+} ($BP^{\cdot+}$)

increased with irradiation time as shown in Fig. 4. In this system, the photoinduced electron transfer from the photoexited triplet state of ZnTPPS (^{3}ZnTPPS*) to BP^{2+} proceeded. The oxidation potential for TEOA was reported to be 0.93 V (*vs* Ag/AgCl) [31] Energy level of first singlet state for ZnTPPS was estimated to be 2.07 eV using the average value of the frequencies of the longest wavelength of the absorption maxima and the shortest wavelength of the fluorescence emission maxima (606 nm by exciting the ZnTPPS at 422 nm). The redox potentials of the exited triplet state of ZnTPPS, *E* ($ZnTPPS^+$/ ^{3}ZnTPPS*) and *E* (^{3}ZnTPPS* / $ZnTPPS^-$) were reported to be -0.75 and 0.45 V, respectively [32,33]. Thus, the reduction efficiency of BP^{2+} with the visible-light sensitization of ZnTPPS depends on the redox potential of BP^{2+}. By using DB^{2+} with the lowest redox potential among BP^{2+}s, the concentration of $DB^{\cdot+}$ produced was estimated to be 80 μM after 180 min irradiation.

3.4. Visible light-induced formic acid synthesis from CO_2 with ZnTPPS, 2,2'-bipyridinium salt derivatives and FDH

Photochemical formic acid synthesis from CO_2 was investigated by adding FDH to the BP^{2+} photoreduction system using photosensitization of ZnTPPS in the presence of TEOA. When the reaction mixture containing ZnTPPS, BP^{2+}, TEOA and FDH in CO_2 saturated sodium pyrophosphate buffer was irradiated with visible light at 30 ˚C, formic acid production was observed with irradiation

time as shown in Fig. 5. The formic acid production from CO_2 with the visible-light sensitization ZnTPPS also depends on the redox potential of BP^{2+}. In contrast, no formic acid production was observed under dark or in the absence of CO_2 condition. Moreover, no formic acid production also was observed in the absence of FDH.

These results indicate that the photochemical and enzymatic synthesis of formic acid from CO_2 with FDH via the photoreduction of BP^{2+} using ZnTPPS photosensitization.

Next let us focus on the interaction between the reduced form of BP^{2+} and FDH activity. Kodaka and Kubota reported that effect of chemical structures of various BP^{2+} on the photochemical and enzymatic formic acid synthesis from CO_2 with the system consisting of TEOA, $[Ru(bpy)_3]^{2+}$, BP^{2+} and FDH [24]. In this system, the formic acid production was order of TB^{2+}, MV^{2+}, and QB^{2+} after 7 h irradiation. TB^{2+} was the most active electron carrier and has a redox potential located between those of $*[Ru(bpy)_3]^{2+}/[Ru(bpy)_3]^{3+}$ and $CO_2/HCOO^-$. For the system using ZnTPPS, the redox potentials of ^{3}ZnTPPS* / $ZnTPPS^+$ and $CO_2/HCOO^-$ were estimated to be -0.75 and -0.61 V, respectively. DB^{2+} was the most active electron carrier and has a redox potential located between those of ^{3}ZnTPPS* / $ZnTPPS^+$ and $CO_2/HCOO^-$.

Moreover, relationship among the dihedral angle of reduced form of BP^{2+}, the redox potential of BP^{2+} and the conversion of CO_2 to formic acid with the system consisting of $[Ru(bpy)_3]^{2+}$ and FDH was studied [24]. The dihedral angles of reduced form of DB^{2+}, TB^{2+}, QB^{2+}

and DM^{2+} calculated by molecular mechanics method (MMX) were estimated to be about 21, 37, 45, and 55˚, respectively [24]. Thus, the reduced form of BP^{2+} with small dihedral angle acts as an effective electron carrier for FDH.

As the DB^{2+} is easy to reduce compared with the other BP^{2+}s and its reduced form has small dihedral angle, thus, effective formic acid production is observed by using DB^{2+} in the system using ZnTPPS as a photosensitizer. Although the reduction efficiency of MV^{2+} was higher than that of TB^{2+}, the formic acid production using MV^{2+} was lower than that of using TB^{2+}. This result showed that the affinity of reduced form of TB^{2+} for FDH was higher than that of reduced form of MV^{2+}.

4. Conclusion

In this work, effect of chemical structures of 2,2'-bipyridinium salts as the electron carrier molecules on the visible-light induced conversion of CO_2 to formic acid with the system consisting of ZnTPPS and FDH in the presence of TEOA as an electron donor molecule was investigated. In the BP^{2+} photoreduction with the visible-light sensitization of ZnTPPS, the reduction efficiency of BP^{2+} depends on the redox potential of BP^{2+} and effective photoreduction was observed using DB^{2+} with the lowest redox potential among BP^{2+}s. In the formic acid production from CO_2 with the system consisting of TEOA, ZnTPPS, BP^{2+} and FDH, formic acid production yield depends on the redox potential of BP^{2+} and the dihedral angle of the reduced form of BP^{2+}, and effective formic

acid production using DB^{2+} with the lowest redox potential and smallest dihedral angle also was observed compared with the other BP^{2+}s.

Acknowledgment

This work was partially supported by Precursory Research for Embryonic Science and Technology (PRESTO, Japan Science and Technology Agency JST), Grants-in-Aid for Scientific Research (C) (Japan Society for the Promotion of Science) (23560947), and Grant-in-Aid for Scientific Research on Innovative Areas "Artificial Photosynthesis (2406)".

References

[1] B. Aurian-Blajeni, M. Halmann, J. Manassen, Solar Energy, 25 (1980)165.

[2] J. Kiwi, K. Kalyanasundaram, M. Grätzel, Struct. Bonding 49 (1982) 37.

[3] J.R. Darwent, P. Douglas, A. Harriman, G. Porter, M.C. Richoux, Coord. Chem., Rev. 44 (1982) 93.

[4] I. Okura, Coord. Chem. Rev., 68 (1985) 53.

[5] I. Okura, Biochimie, 68 (1986) 189.

[6] I. Okura, S. Aono, A. Yamada, J. Phys. Chem. 89 (1985) 1593.

[7] Y. Amao, I. Okura, J. Mol. Catal. A: Chem., 103 (1995) 69.

[8] Y. Amao, I. Okura, J. Mol. Catal. A: Chem., 105 (1996) 125.

[9] T. Itoh, H. Asada, K. Tobioka, Y. Kodera, A. Matsushima, M. Hiroto, H. Nishimura, T. Kamachi, I. Okura, Y. Inada, Bioconjugate Chem., 11 (2000) 8.

[10] Y. Amao, I. Okura, "Photocatalysis-Science and Technology" KODANSHA-Springer 2002

[11] A. Harriman, G. Porter, M.-C. Richoux, J. Chem. Soc., Faraday Trans.2, 77(1981) 833.

[12] I. Okura, M. Takeuchi, N. Kim-Thuuan, Photochem. Photobiol., 33(1981) 413.

[13] I. Okura, M. Takeuchi, S. Kusunoki, S. Aono, Inorg. Chim. Acta. 63(1982) 157.

[14] I. Okura, N. Kaji, S. Aono, T. Kita, A. Ymada, Inorg. Chem., 24 (1985) 451.

[15] T. Kamachi, T. Hiraishi, I. Okura, Chem. Lett., 1995, 33.

[16] Y. Tomonou, Y. Amao, Int. J. Hydrogen Energy, 29 (2004)159.

[17] Y. Tomonou, Y. Amao, Biometals 15 (2002) 391.

[18] Y. Tomonou, Y. Amao, Biometals 16 (2003) 419.

[19] R. Miyatani, Y. Amao, Photochem. Photobiol. Sci., 3(2004) 681.

[20] D. Mandler, I. Willner, J. Chem. Soc., Perkin Trans., 2 (1988) 997.

[21] I. Willner, D. Mandler, J. Am. Chem. Soc., 111(1989)1330.

[22] I. Willner, N. Lapidot, A. Riklin, R. Kasher, E. Zahavy, E. Katz, J. Am. Chem. Soc., 116 (1994)1428.

[23] I. Willner, I. Willner, N. Lapidot, J. Am. Chem. Soc., 112 (1990) 6438.

[24] M. Kodaka, Y. Kubota, J. Chem. Soc., Perkin Trans., 2 (1999) 891.

[25] R. Miyatani, Y. Amao, Biotechnol. Lett., 24(2002)1931.

[26] R. Miyatani, Y. Amao, J. Mol. Catal. B. Enzym., 27(2004)121.

[27] R. Miyatani, Y. Amao, J. Jpn. Petrol. Inst., 47 (2004) 27.

[28] I. Tsujisho, M. Toyoda, Y. Amao, Catal. Commun, 7 (2006) 173.

[29] Y. Amao, T. Watanabe, Chem. Lett., 33 (2004)1544.

[30] Y. Amao, T. Watanabe, Appl. Catal. B. Environment., 86(2009)109.

[31] S. Karastogianni, S. Girousi, Sensing in Electroanalysis Vol. 8 (K. Kalcher, R. Metelka, I. Švancara, K. Vyt ř as; Eds.), pp. 241-252. 2013/2014 University Press Centre, Pardubice, Czech Republic.

[32] M. Kaneko, K. Suzuki, E. Ebel, D. Wöhrle, Macromol. Symp. 204 (2003) 71.

[33] K. Kalyanasundaram, M Nerman-Spallart, J. Phys. Chem. 86 (1982) 5163.

Captions to Figures

Fig. 1. Chemical structures of bipyridinium salt derivatives.

Fig. 2. Photochemical and enzymatic synthesis of formic acid from CO_2 with the system consisting of TEOA, ZnTPPS, bipyridinium salt (BP^{2+}) and FDH.

Fig. 3. UV-vis absorption spectrum of ZnTPPS in 3.0 ml of 1.0 mM sodium pyrophosphate buffer (pH 7.4).

Fig. 4. Time dependence of reduced bipyridinium salt derivative production under steady state irradiation with visible light using a 250 W halogen lamp at a distance of 3.0 cm. The solution contained ZnTPPS (10 μM), 2,2'-bipyridinium salt derivative (0.1 mM) and TEOA (0.3 M) in 3.0 ml of 1.0 mM sodium pyrophosphate buffer (pH 7.4).

Fig. 5 Time dependence of formic acid production under steady state irradiation with visible light using a 250 W halogen lamp at a distance of 3.0 cm. The solution contained ZnTPPS (10 μM), 2,2'-bipyridinium salt derivative (0.1 mM), TEOA (0.3 M) and FDH (9.3 μM) in 3.0 ml of 1.0 mM CO_2 saturated sodium pyrophosphate buffer (pH 7.4).

Scheme 1-1 Synthesis procedure of 1,1’-alkyl-2,2’-bipyridinium salt.

Scheme 1-2 Synthesis procedure of 1,1’-dimethyl-2,2’-bipyridinium salt.

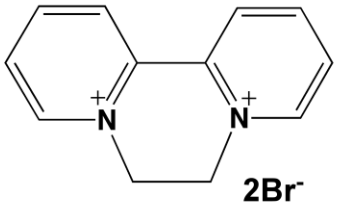

1,1'-Ethylene - 2,2'- bipyridinium dibromide
(DB^{2+})

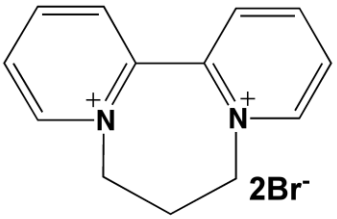

1,1'-Trimethylene - 2,2'- bipyridinium dibromide
(TB^{2+})

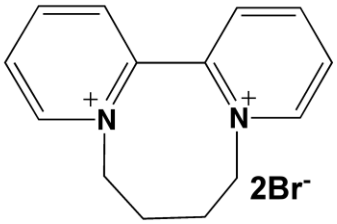

1,1'-Tetramethylene - 2,2'- bipyridinium dibromide
(QB^{2+})

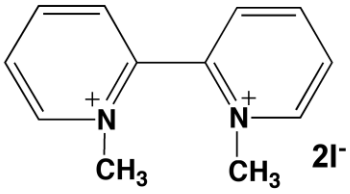

1,1'-Dimethyl - 2,2'- bipyridinium diiodide
(DM^{2+})

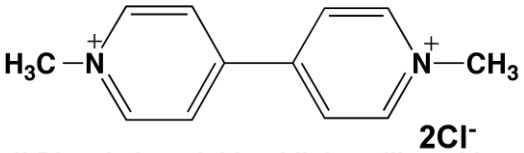

1,1'-Dimethyl - 4,4'- bipyridinium dibromide
(MV^{2+})

Fig. 1

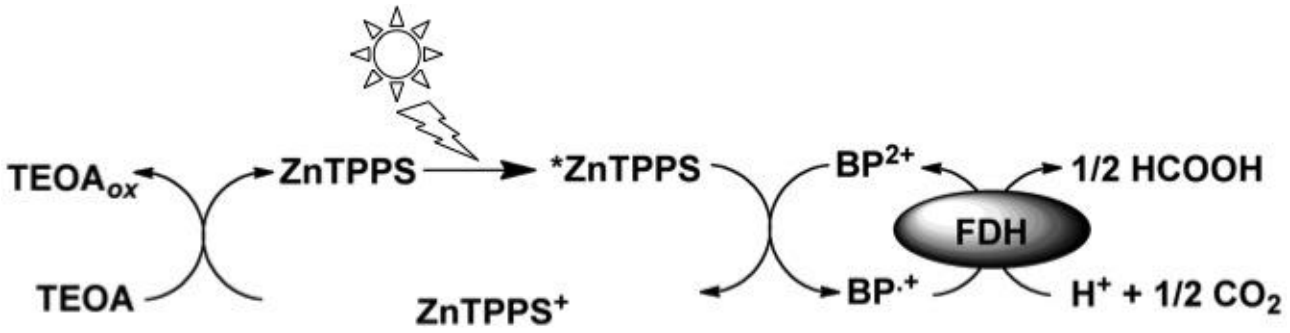
TEOA$_{ox}$
ZnTPPS
*ZnTPPS
BP^{2+}
1/2 HCOOH
FDH
TEOA
ZnTPPS^{+}
BP$^{\cdot+}$
H^{+} + 1/2 CO$_2$

Fig. 2

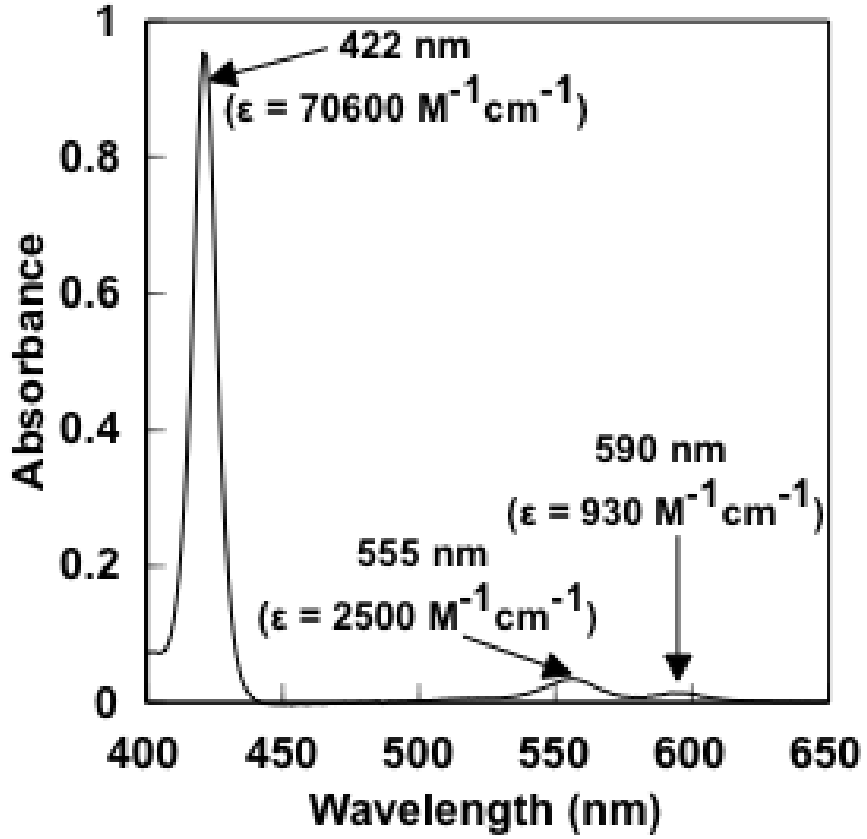
422 nm
(ε = 70600 M-1cm-1)
590 nm
(ε = 930 M-1cm-1)
555 nm
(ε = 2500 M-1cm-1)
Absorbance
Wavelength (nm)
0
0.2
0.4
0.6
0.8
1
400
450
500
550
600
650

Fig. 3

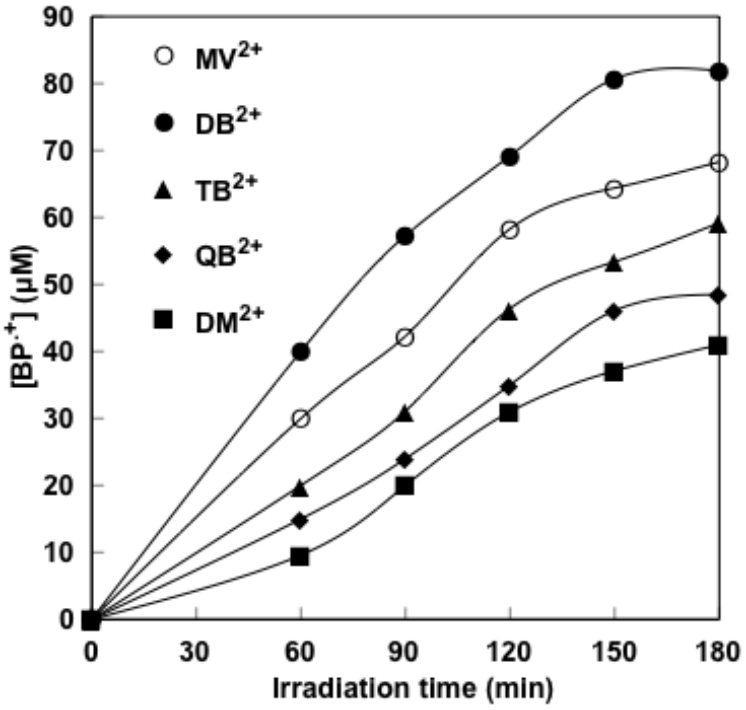
90
80
70
60
50
40
30
20
10
0
0
30
60
90
120
150
180
[BP·+] (μM)
Irradiation time (min)
MV2+
DB2+
TB2+
QB2+
DM2+

Fig. 4

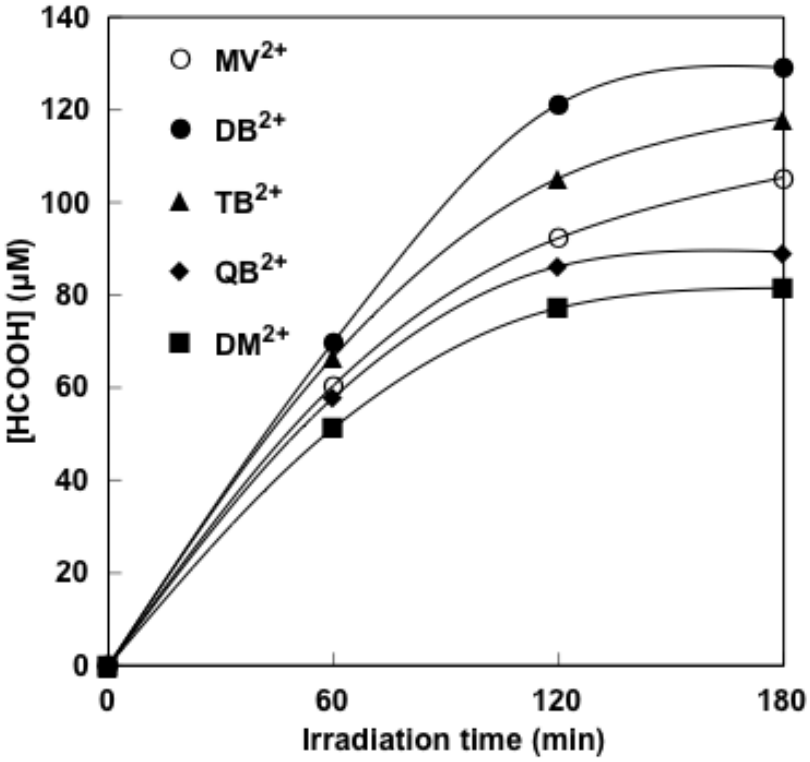
140
120
100
80
60
40
20
0
[HCOOH] (μM)
MV2+
DB2+
TB2+
QB2+
DM2+
0
60
120
180
Irradiation time (min)

Fig. 5

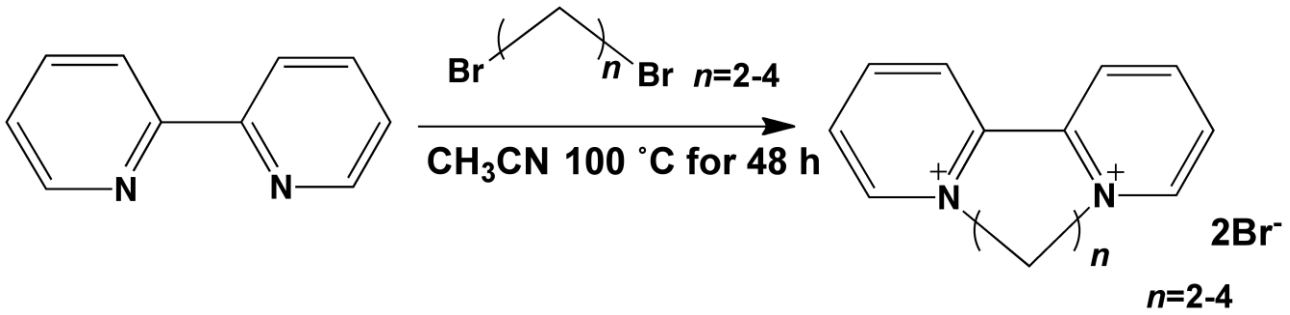

Scheme 1-1

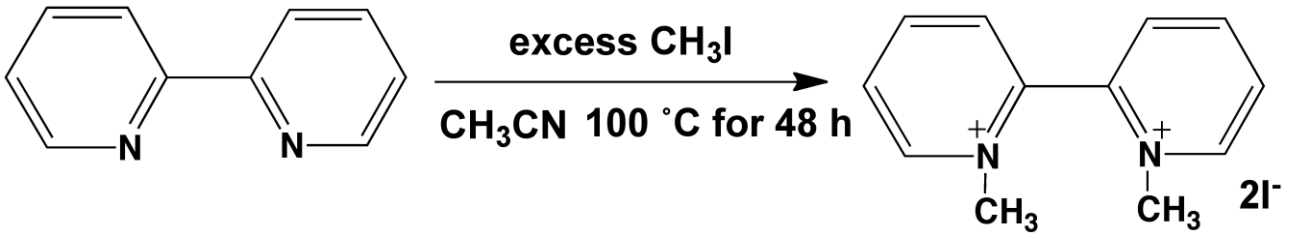

Scheme 1-2